Syntheses, Structures and Solution Dynamics of Anionic 5-Coordinate Pt(II) Complexes with Halide

Seichi Okeya,* Masato Hashimoto, Takahito Matsuo,† Kimiko Yamanaka,† Tetsuya Sumino,† Hiroshi Hashimoto,††
Nobuko Kanehisa,†† and Yasushi Kai*††
Department of Material Science and Chemistry, Faculty of Systems Engineering, Wakayama University, Sakaedani, Wakayama 640-8510
†*Faculty of Education, Wakayama University, Sakaedani, Wakayama 640-8510*
††*Department of Applied Chemistry, Faculty of Engineering, Osaka University, Suita, Osaka 565-0871*

(Received February 2, 1998; CL-980074)

Five-coordinate anionic complexes, [Pt(hfac)$_2$X]$^-$ (X = Cl, Br, I), were prepared by reaction of [Pt(hfac)$_2$] and [PPh$_4$]X in CH$_2$Cl$_2$. A distorted square pyramidal structure was revealed by the X-ray analysis. The variable-temperature ^{1}H and ^{19}F NMR spectra of these complexes were explained by two independent dynamic motions in solution, which were considered good models for the ligand exchange and *cis-trans* isomerization reactions.

The five-coordinate d^8 metal complex[1] is important as an intermediate in the associative ligand substitution and isomerization reactions of four-coordinate square planar complex. [M(hfac)$_2$] (M = Pd, Pt, hfac = hexafluoroacetylacetonate) reacts with tertiary phosphine(L) to afford a distorted square pyramidal 5-coordinate complex, [M(hfac)$_2$L], in which the phosphine ligand is in the basal plane.[2,3] Two kinds of twist mechanism have been proposed to account for their dynamic behavior in CDCl$_3$.[3] Here we describe some new anionic 5-coordinate Pt(II) halide complexes.

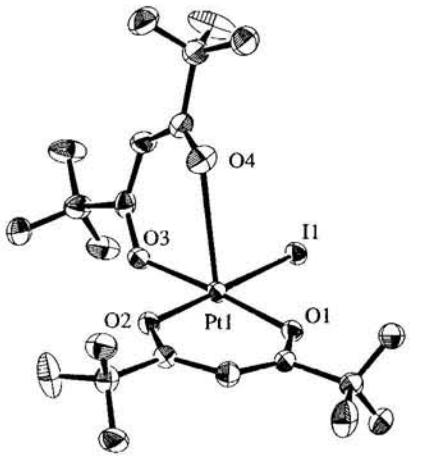

Figure 1. ORTEP drawing of **1c** (PPh$_4$$^+$ is omitted).

Table 1. Selected bond lengths (Å).

	1b	**1c**
Pt1-O1	1.995(5)	1.984(6)
Pt1-O2	2.023(3)	2.032(7)
Pt1-O3	2.019(5)	2.008(7)
Pt1-O4	2.951(5)	2.942(8)
Pt1-X1	2.3980(5)	2.5675(8)

A CH$_2$Cl$_2$ solution of [PPh$_4$]Cl was added to a CH$_2$Cl$_2$ solution containing one equivalent of [Pt(hfac)$_2$]. Diethyl ether and n-pentane were added to the resulting mixture, and it was kept in a refrigerator to allow the deposition of red crystals of [PPh$_4$][Pt(hfac)$_2$Cl] **1a** (yield; 58%).[4] [PPh$_4$][Pt(hfac)$_2$X] (**1b**: X = Br, **1c**: X = I) were also isolated in a similar fashion as red crystals (yield; 77% for **1b** and 71% for **1c**). A distorted square pyramidal structure with the halide ligand in the basal plane was determined by single crystal X-ray analysis (for **1c** in Figure 1).[5] Selected bond lengths are listed in Table 1. The apical oxygen donor atom(O4) has a weak bonding interaction with the metal because the Pt1-O4 distances are 2.9 Å. The position of O4 deviates moderately from the regular square pyramid (< O3-Pt-O4 are 75~76°). The Pt atom is almost on the mean basal plane. In solution, complex **1a** rearranged gradually to 4-coordinate [Pt(hfac)(hfac-*O*)Cl]$^-$ **2a**, in which the apical oxygen was freed from a coordination site.[6] When one equivalent of halide reacted with complex **1** or **2**, [Pt(hfac)X$_2$]$^-$ **3** was formed.[7] Moreover, when more than two equivalents of halide were added to the solution of **1**, a salt of [PtX$_4$]$^{2-}$ or [Pt(μ-X)X$_2$]$_2$$^{2-}$ was precipitated. Thus complexes **1** and **2** are intermediates in the substitution reaction of hfac by halide ligands. The variable-temperature ^{1}H and ^{19}F NMR (Figure 2) of **1** were recorded. At sufficiently low temperatures two singlets of hfac-CH in ^{1}H NMR and four singlets of CF$_3$ in ^{19}F NMR were observed. At elevated temperatures these signals broadened and sometimes coalesced. This dynamic behavior is accounted for by two independent intramolecular processes; these proceed via trigonal bipyramidal transition states (Scheme 1).[3] The rate of hfac exchange between basal/basal and apical/basal positions (Path B) monitored by ^{1}H NMR is in the order **1a** < **1b** < **1c**,[8] reflecting trans effect of X. Interestingly the nature of the signal deformation in the ^{19}F NMR depends on the type of halide ligand (Figure 2). On gradual elevation of the temperature both outer signals assigned to the basal/apical chelate (*ap* and *c-2*) of **1a** broadened first and the central two signals assigned to the basal/basal chelate (*tr* and *c-1*) broadened next, in spite of the larger signal separation for the basal/apical chelate. These results suggest that k$_A$ should be larger than k$_B$ for **1a**.[9] On the other hand the four CF$_3$ signals of **1c** changed to two signals at equal rates; the lower field signal due to the exchange of O^b and O^d, and the other to that of O^a and O^c (Path B). For **1c** these two signals broadened again at 40 °C (Path A). The dynamic ^{19}F NMR spectra of **1b** behaved like those of **1c**. These results indicate that k$_B$ is much larger than k$_A$ for the bromide and iodide

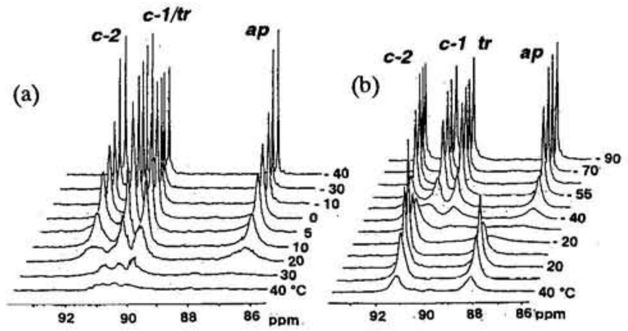

Figure 2. Variable-temperature ^{19}F NMR spectra of (a) $[Pt(hfac)_2Cl]^-$ **1a** and (b) $[Pt(hfac)_2I]^-$ **1c** in CD_2Cl_2 (tentative assignment).

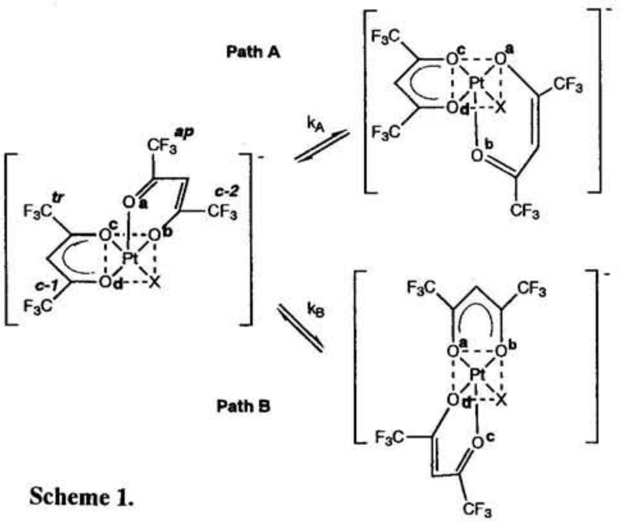

Scheme 1.

complexes, being similar to the phosphine analogue.[3] From a rough estimate, the rate of oscillating motion of one hfac (Path A) is in the order **1a** > **1c**.[10] It is very significant that the reverse of the trans effect was found as a "cis" effect for the halide ligand, whether the effect is not large. Path A and Path B are good models for the self-exchange reaction of oxygen donor ligand at the *cis* and *trans* positions, respectively, to the X^- ligand in square planar Pt(II) complex, for example, $[PtX(H_2O)_3]^+$ in aqueous solution Moreover a successive process of Path A and Path B brings *cis-trans* isomerization. It would be predicted that the rate of isomerization is not sensitive to the kind of halide ion.[11]

S.O. is gratful to the Ministry of Education, Science and Culture for Grant-in-aid for Scientific Research, No. 08454210.

References and Notes

1 G. Aullon and S. Alvarez, *Inorg. Chem.*, **35**, 3137 (1996).

2 A. R. Siedle, R. A. Newmark, and L. Pignolet, *J. Am. Chem. Soc.*, **104**, 6584 (1982).

3 S. Okeya, T. Miyamoto, S. Ooi. Y. Nakamura, and S. Kawaguchi, *B. C. S. Jpn.*, **57**, 395 (1984).

4 Satisfactory analytical data were obtained for **1a**, **1b**, and **1c**. **1a**: IR (KBr); 1696s, 1588s, 1563vs, 1532s (ν(CO)). ^1H NMR (CD_2Cl_2, -40 °C, 90 MHz); δ 5.91 (1H), 6.20 (1H, *J*(Pt-H) = 11 Hz). ^{19}F NMR (CD_2Cl_2, -40 °C, 84 MHz, Ref; External C_6F_6); δ 86.76, 90.28 (*J*(Pt-F) = 13 Hz), 90.84 (*J*(Pt-F) = 13 Hz), 91.73 (*J*(Pt-F) = 6 Hz). **1b**: IR; 1684s, 1587s, 1559vs, 1522s (ν(CO)). ^1H NMR (CD_2Cl_2, -40 °C); δ 5.89 (1H), 6.20 (1H). ^{19}F NMR (CD_2Cl_2, -60 °C); δ 86.86, 90.36 (*J*(Pt-F) = 12 Hz), 90.94 (*J*(Pt-F) = 13 Hz), 91.98. **1c**: IR; 1689s, 1593s, 1567vs, 1522s (ν(CO)). ^1H NMR (CD_2Cl_2. -90 °C); δ 5.90 (s, 1H), 6.28 (s, 1H). ^{19}F NMR (CD_2Cl_2, -90 °C); δ 87.05, 90.41, 91.11, 92.40.

5 **1b**: $C_{34}H_{22}F_{12}BrPPtO_4$, *F.W.* = 1028.5, triclinic, $P\bar{1}$, a = 11.842(2) Å, b = 14.172(4) Å, c = 11.858(3) Å, α = 113.10(3)°, β = 101.78(4)°, γ = 81.22(2)°, V = 1786(1) Å^3, Z = 2, D_c = 1.912 g cm^{-3}, $\mu(MoK\alpha)$ = 51.79 cm^{-1}, R = 0.036 for 8292 reflections ($I > 4.0\sigma(I)$). **1c**: $C_{34}H_{22}F_{12}IPPtO_4$, F.W. = 1075.5, triclinic, $P\bar{1}$, a = 11.747(3) Å, b = 14.128(3) Å, c = 11.557(3) Å, α = 102.85(2)°, β = 103.44(1)°, γ = 85.99(2)°, V = 1818.4(8) Å^3, Z = 2, D_c = 1.964 g cm^{-3}, $\mu(MoK\alpha)$ = 48.34 cm^{-1}, R = 0.056 for 7823 reflections ($I > 4.0\sigma(I)$). Diffraction data were collected on a Rigaku RAXIS-CS imaging plate area detector with graphite-monochromated Mo*K*α radiation at -190 °C. All calculations were performed using the teXsan Crystallographic Software package of Molecular Structure Corporation. Though **1a** was also subjected to the X-ray analysis, satisfactory result has not been obtained so far due to the poor quality of the crystal.

6 Synthesis of **2a**; a CH_2Cl_2 solution of $[Pt(hfac)_2]$ was added to a CH_2Cl_2 solution of two equivalents of $[AsPh_4]Cl$ at around -30 °C. Et_2O and n-pentane were added to the resulting mixture to deposit an orange precipitate, which was filtered and washed with Et_2O (Yield; 72%). Anal. Found: C, 40.45; H, 2.29%. Calcd for $C_{34}H_{22}ClF_6AsPt$: C, 39.73; H, 2.16%. IR (KBr); 1687s, 1591s, 1558vs, 1521s (ν(CO)). ^1H NMR ($CDCl_3$, -10 °C, 90 MHz); δ 6.18 (1H, hfac-*O,O'*), 7.03 (1H, hfac-*O*). ^{19}F NMR ($CDCl_3$, -40 °C, 84 MHz); δ 89.9, 93.2(*J*(Pt-F) = 10 Hz), 93.6, 96.9 (*J*(Pt-F) = 15 Hz).

7 Synthesis of **3**(X = Cl); $[Pt(hfac)_2]$ and two equivalents of $[PPh_4]Cl$ were dissolved in CH_2Cl_2 at room temperature. n-Pentane was added to this solution, which was left in a refrigerator. The resulting brown microcrystals were filtered off and washed with Et_2O and H_2O (Yield; 81%). The bromide and iodide analogues were also prepared. Anal. Found: C, 54.46; H, 3.36%. Calcd for **3**·$[PPh_4]$hfac ($C_{58}H_{42}O_4P_2Cl_2F_{12}Pt$): C, 54.84; H, 3.33%. IR (KBr); 1669vs (hfac$^-$), 1622s, 1586m, 1552vs, 1526s, 1510m (ν(CO)). ^1H NMR ($CDCl_3$, 90 MHz); δ 5.46 (hfac$^-$), 5.96 (hfac-*O,O'*). ^{19}F NMR ($CDCl_3$, 84 MHz); δ 90.65 (hfac$^-$), 92.89 (hfac-*O,O'*).

8 Coalescence temperatures were ca. 30 for **1a**, 0 for **1b** and -50 °C for **1c**, respectively($k_B \approx 30\ s^{-1}$).

9 k_A value was calculated to be four times higher than k_B for **1a**. (For example; $k_A \approx 40\ s^{-1}$ and $k_B \approx 11\ s^{-1}$ at 5 °C)

10 Same rate constant($k_A \approx 30\ s^{-1}$) was evaluated for **1a** at 0 °C and for **1c** at 20 °C.

11 The rate-determining step of *cis-trans* isomerization is Path B for **1a**, and the rate is similar in magnitude to that (Path A) of **1c**.